

# Discovery of an ionized Fe-K edge in the $z=3.91$ Broad Absorption Line Quasar APM 08279+5255 with *XMM-Newton*

G. Hasinger<sup>1</sup>, N. Schartel<sup>2</sup>, and S. Komossa<sup>1</sup>

<sup>1</sup>*Max-Planck-Institut für extraterrestrische Physik, Postfach 1312, D-85741 Garching, Germany*

<sup>2</sup>*XMM-Newton Science Operation Center, European Space Agency, Villafranca del Castillo, Apartado 50727, E-28080 Madrid, Spain*

## ABSTRACT

Recent *XMM-Newton* observations of the high-redshift, lensed, broad absorption line (BAL) quasi-stellar object APM 08279+5255, one of the most luminous objects in the universe, allowed the detection of a high column density absorber ( $N_H \approx 10^{23} \text{ cm}^{-2}$ ) in the form of a K-shell absorption edge of significantly ionized iron (Fe XV - XVIII) and corresponding ionized lower-energy absorption. Our findings confirm a basic prediction of phenomenological geometry models for the BAL outflow and can constrain the size of the absorbing region. The Fe/O abundance of the absorbing material is significantly higher than solar (Fe/O = 2–5), giving interesting constraints on the gas enrichment history in the early Universe.

*Subject headings:* quasars: individual (APM 08279+5255) – quasars: absorption lines – X-rays: galaxies

## 1. Introduction

Absorption Line (BAL) Quasi-stellar Objects (QSOs) are a key to understand the geometry and physical state of the medium in the immediate vicinity of accreting supermassive black holes. A new unified model (Elvis 2000) indicates that a significant fraction of the matter accreted into the region of the compact object is flowing out again. On either side of the accretion disk it should form a funnel-shaped shell, in which the outflowing gas is ionized and accelerated to velocities of 0.05-0.1c by the powerful radiation force of the central object. If the observer's inclination is favorable, this flow intercepts the line of sight with a large column density and produces the blue-shifted broad UV absorption line features observed in about 10% of all QSOs. However, the UV/optical spectra sample only a minor fraction

of the total column density of the flow, which is predicted to be highly ionized so that it mainly absorbs X-rays.

APM 08279+5255 is an exceptionally luminous Broad Absorption Line (BAL) QSO at redshift  $z=3.91$  (Irwin et al., 1998), coincident with an IRAS Faint Source Catalogue object and was also detected at  $850 \mu\text{m}$  with SCUBA, implying an apparent far-infrared luminosity of  $> 5 \times 10^{15} L_{\odot}$  (Lewis et al., 1998). The object is strongly lensed (Ledoux et al., 1998; Ibata et al., 1999; Egami et al., 2000), with a magnification factor of 50-100, but even taking this magnification factor into account, the object is still among the most luminous in the Universe. The low resolution discovery spectrum of APM 08279+5255 showed a broad absorption trough (BAL) on the blue side of  $\text{Ly}_{\alpha}$ . An excellent high resolution optical spectrum was obtained with HIRES at the Keck telescope (Ellison et al., 1999) and a detailed study of the physical conditions in the broad absorption line flow of the QSO (Srianand & Petitjean, 2000) came to the conclusion, that the corresponding gas stream, outflowing with velocities up to  $12000 \text{ km s}^{-1}$ , is heavily structured and highly ionized.

In this paper we report X-ray observations of APM 08279+5255 with *XMM-Newton* obtained in October 2001 and April 2002, where we detected an ionized Fe K edge in the continuum of the QSO which is very likely related to the UV broad absorption line flow. In section 2 we present the X-ray observations and analysis. In section 3 we discuss the results. Throughout this paper we use a Hubble constant of  $50 \text{ km s}^{-1} \text{ Mpc}^{-1}$  and a deceleration parameter  $q_0 = 0.5$ .

## 2. X-ray Observations and analysis

The first X-ray observation of APM 08279+5255 was taken on October 11, 2000 with the *Chandra* observatory (Gallagher et al., 2002). *XMM-Newton* observed APM 08279+5255 for 15 ksec on October 30, 2001 in good background conditions. The EPIC spectrum revealed a tantalizing absorption feature around 1.5 keV, close to the energy expected from highly redshifted iron, either associated with the object itself or with intervening material. Unfortunately the statistical quality of the data did not allow more quantitative analysis. A proposal for director's discretionary time for a significantly longer observation (100 ksec) was accepted by the *XMM-Newton* project scientist and executed on April 28–29, 2002. Table 1 gives details for the *XMM-Newton* and *Chandra* observations.

The XMM data were analyzed using the latest version of the standard analysis software *SAS 5.0*. The EPIC pn-CCD detector detected the source with an average count rate of  $\sim 0.19 \text{ cts s}^{-1}$  and  $\sim 0.15 \text{ cts s}^{-1}$ , in the XMM1 and XMM2 observation, respectively. Within

each of the observations there is no significant time variability detected. Fig. 1 shows the normalized pn–CCD counts spectrum of the source from the 100 ksec XMM2 observation. The source is clearly detected out to 12 keV (almost 60 keV in the restframe of the quasar!). Using *xspec version 11.1.0*, we fitted the combined pn–CCD and MOS–CCD spectra and in all fits included a neutral absorption with the Galactic  $N_H$  value fixed to  $4 \times 10^{20} \text{ cm}^{-2}$ . Following Gallagher et al. (2002), we first assumed a simple power law spectrum with an intrinsic cold gas absorber in the rest frame of the QSO ( $z=3.91$ ). The two *XMM–Newton* (EPIC pn+MOS) and one *Chandra* (ACIS-I) dataset can be fit with the same model and, apart from a  $\sim 20\%$  flux decrease between the first and the last observation, the spectral fit parameters are consistent between the three datasets. The best fit values for all three datasets are given in Table 2.

The spectral fit residuals of the 100 ksec XMM2 observation, however, show systematic deviations across the whole spectral range (Fig. 1). The fit is statistically unacceptable (reduced  $\chi^2 = 1.45$  for 126 degrees of freedom), the most significant deviation is an edge-like feature around 1.55 keV, corresponding to roughly 7.7 keV in the rest frame of the object. There is no evidence for an emission line associated with the K edge: the upper limit for the equivalent width of a narrow emission line in the rest-frame energy range 6.4–6.9 keV is about 110 eV, much lower than those found e.g. from ionized reflection disk models. We therefore interpret the observed spectral feature as an absorption edge due to ionized iron in the BAL flow of APM 08279+5255. Indeed, if we include an additional absorption edge in the spectral model we obtain a highly significant improvement of the fit ( $\Delta\chi^2 = -87$  for two additional parameters) for the XMM2 dataset with an edge energy of  $E_{edge} = 7.7 \pm 0.1 \text{ keV}$  and an optical depth of  $\tau = 0.46 \pm 0.07$ . An improved fit is also obtained for the XMM1 observation, with independently determined edge parameters consistent with the XMM2 dataset. The *Chandra* spectrum (CXO1), which is of lower signal to noise, does not require an edge, but if it is included, the energy and depth are fully consistent with the XMM values (see Table 2).

Fig. 2 shows  $\chi^2$  confidence contours for the edge energy versus the optical depth derived from the XMM2 data in comparison with the K edge energy expected for different ionic species of Fe. The best-fit parameters are compatible with Fe XVII, with a range from Fe XV to Fe XVIII, indicating significant ionization of iron. Assuming the absorption cross section of the Fe XVII K edge ( $2.7 \times 10^{-20} \text{ cm}^2$ ), computed using the analytical fits of Verner & Yakovlev (1995), we can determine the column density of ionized Fe to  $N_{Fe} \approx 1.7 \times 10^{19} \text{ cm}^{-2}$ , relatively independent of the ionization state of iron. Assuming solar abundances, this would correspond to an effective hydrogen column density of  $N_H \approx 6 \times 10^{23} \text{ cm}^{-2}$ , about a factor of 7 larger than the hydrogen column density derived by fitting a cold, neutral absorber to the low–energy cutoff of the spectrum.

The fit of a neutral absorber in conjunction with a highly ionized Fe-K edge is, however, physically not meaningful. If Fe is partly ionized, most of the lighter elements will also be ionized and therefore will absorb the X-ray continuum less strongly. Indeed, the detailed treatment of the high resolution UV/optical spectrum of this source indicates a total neutral hydrogen column density not much larger than several times  $10^{18} \text{ cm}^{-2}$  (Srianand & Petitjean, 2000). However, edges of hydrogen- and helium-like ions of lower- $Z$  elements (O, Ne, Mg, Si and S) as well as the Fe L edge will absorb lower energy photons and can mimic a cold gas absorber (Schartel et al. 1997, Komossa 1999). To estimate their effect, we have scaled the column density for these elements to the measured  $N_{Fe}$ , assuming solar abundance ratios. Including these edges into the model spectrum produces significantly more low-energy absorption than observed in the data. Indeed, reducing the K edge depth of lower- $Z$  elements by a factor of 5, while leaving the depth of the Fe L edge at the predicted depth of 8.7 gives a very good approximation to the lower-energy absorption observed in APM 08279+5255. This indicates a high overabundance of iron with respect to lower- $Z$  elements.

A more quantitative treatment has to include the photoionization of the BAL flow and the balance between different ionization states of the elements. Therefore we fitted a power law model, folded through the Galactic  $N_H$  and an ionized absorber (model *absori* contained in *xspec*, Done et al., 1992). We obtain an excellent fit to the XMM2 data with a reduced  $\chi^2$  of 1.09. Fig. 3 shows confidence intervals for the interesting parameters in the *absori* fit. The equivalent hydrogen column density is in the range  $N_H = (1.0 \pm 0.2) \times 10^{23} \text{ cm}^{-2}$  somewhat higher than the neutral hydrogen column densities in Table 1, but an iron overabundance of  $Fe/O=2-5$  is required to take care of the observed Fe-K edge in relation to the lower-energy absorption by O, Ne, Mg K edges and the Fe L edge. There is a correlation between these two parameters in the sense that the total Fe column density can be determined to  $N_{Fe} \approx 1.5 \times 10^{19} \text{ cm}^{-2}$ , rather independent from the Fe overabundance and consistent with the value obtained by just fitting an edge (see above).

For a more detailed study, we have constructed grids of photoionization models using the code *Cloudy* (Ferland 1993), varying the gas column density  $N_{Fe}$  and the ionization parameter  $U$  until we obtain an Fe-K ionization level and optical depth consistent with the observed edge (see below).  $U$  is defined as  $U = \frac{Q}{4\pi r^2 n_H c}$ , where  $Q$  is the rate of ionizing photons above the Lyman limit. As input continuum we chose a mean AGN continuum spectrum, consisting of piecewise powerlaws from the radio to the gamma-ray region with, in particular,  $\alpha_{uv-x} = -1.4$  in the EUV and an observed  $\Gamma_x = -2.0$ . The results of this analysis are discussed in section 3.1.

### 3. Discussion

For the first time, we have reported the detection of a highly ionized iron edge in the spectrum of a high-redshift BAL quasar. This indicates a very high column density, ionized absorber in the line of sight. Compared to the warm absorbers typically observed in Seyfert galaxies, which are dominated by OVII – OVIII edges of optical depth around unity (see Komossa 1999 and references therein), where strong Fe K edges have not been seen so far, the column density of ionized Fe is considerably higher here and the absorption is very likely associated with the highly ionized BAL flow observed in the UV spectrum of the source.

For the quasar 3C 351 it has been shown, that the associated absorption lines observed in the UV spectrum are most likely produced by the same highly ionized material that is also responsible for the moderate X-ray warm absorber (Mathur et al., 1994). In case of BAL systems, however, interpretation is complicated by the uncertainties in optical depth measurements of the lines: the broad, saturated UV absorption lines from different atomic species do not allow an unambiguous column density determination (e.g., Hamann 1998).

#### 3.1. Implications for X-ray Broad Absorption Line Models

Murray & Chiang (1995) constructed a model in which the BALs arise in an accretion-disk wind driven by line pressure. They predicted that objects with very broad CIV absorption ( $> 5000 \text{ km s}^{-1}$ ) should also show Fe absorption edges in the X-ray regime. This is similar to what we now observe.

The high column density inferred for the X-ray absorber in APM 08279+5255 is also consistent with predictions of the unified model by Elvis (2000). In that model, the UV broad absorption lines occur, when the line of sight to the central object grazes along the funnel-shaped shell of ionized matter thought to constitute the BAL outflow. Using NGC 5548 as reference object in constructing his new unified model, Elvis (2000) predicted a column density of a few  $10^{23} \text{ cm}^{-2}$  for an NGC 5548-like object viewed along the funnel. We find  $\sim 10^{23} \text{ cm}^{-2}$  for APM 08279+5255.

The ionization state of the warm absorber is characterized by the ionization parameter  $U$ . The number rate of ionizing photons,  $Q$ , was estimated from our piecewise powerlaw spectrum with  $\alpha_{\text{uv-x}} = -1.4$  in the EUV and  $\Gamma_x$  as observed, normalized to the observed X-ray flux. We then find  $Q = 1.2 \times 10^{58} k^{-1} \text{ s}^{-1}$ ,  $k$  being the lensing magnification factor. Given the best estimate of the ionization parameter ( $\log U = 0.4$ ) and assuming a density of the absorber of  $\log n = 9.5$  – this is similar to the value suggested by Elvis (2000) to ensure pressure equilibrium with the BELR clouds – we expect a lower limit on the location of the

absorber of  $r \approx 2 \times 10^{18} k^{-1/2}$  cm. A more detailed discussion of the ionized gas properties and consequences for BAL models will be given in a forthcoming paper (G. Hasinger et al. 2002, in prep.).

### 3.2. Relation of X-ray and UV Absorbers and Metal Abundances

Comparison with UV data immediately implies that the X-ray absorber must be dust-free, else the UV continuum would be heavily extinguished. The high degree of ionization of the X-ray absorber is consistent with the UV spectrum which shows strong high-ionization BAL lines including OVI, but relatively weak neutral H absorption.

The UV absorption line data show that the BAL flow is highly structured with saturated absorption bands and thus, contrary to the X-ray absorption edge, cannot determine the total column density in the flow. Based on our best-fit *Cloudy* model, we expect to see UV absorption in e.g., HI, CIV, NV, OVI and NeVIII with column densities on the order of  $N_{\text{HI}} \approx 4 \cdot 10^{16} \text{cm}^{-2}$ ,  $N_{\text{CIV}} \approx 10^{16} \text{cm}^{-2}$ ,  $N_{\text{NV}} \approx 7 \cdot 10^{17} \text{cm}^{-2}$ ,  $N_{\text{OVI}} \approx 6 \cdot 10^{17} \text{cm}^{-2}$ , and  $N_{\text{NeVIII}} \approx 7 \cdot 10^{17} \text{cm}^{-2}$ . The higher metal column densities compared to HI can be traced back to the high degree of ionization of the absorber and do therefore not necessarily indicate chemical overabundances. For a detailed comparison with the UV data, *simultaneous* multi-wavelength observations are required.

No diagnostically valuable, strong Fe lines are present in the UV spectra of BALs. Thus, iron abundance determinations for BALs are still scarce. Fe-K edge X-ray observations therefore nicely supplement UV measurements of other metal species, and allow tests of different scenarios for the origin of the BAL gas.

We find an overabundance of iron of 2–5 times the solar abundance (see Fig. 3). Due to the fact that the measured X-ray absorption is produced mainly by O, Ne, Mg, Si and Fe, this iron overabundance is actually an estimate of  $Fe/O$ . The outflowing material must therefore have already been processed in a starburst environment. Detailed chemical evolutionary scenarios of the emission-line gas in quasars (Hamann & Ferland 1993) predict the iron enrichment that depends mostly on the lifetime of supernova Type Ia precursors, leading to an expected delay of  $\sim 1$  Gyr until  $Fe/O$  reaches solar values. Fe measurements in high- $z$  objects, like APM 08279+5255, therefore (1) are of profound relevance for understanding the early star formation history of the universe and (2) provide important constraints on cosmological models. Assuming an Fe abundance of APM 08279+5255 of at least solar, we can place severe constraints on some of the enrichment models of Hamann & Ferland (1993; their Fig. 1). Furthermore, at the redshift of  $z \approx 4$  the age of the universe is a little

less than 1 Gyr (for  $q_0=0.5$ ), which compares to the timescale of  $\sim 1$  Gyr necessary to enrich  $Fe/O$  up to the solar value. Given that we find strong indications of a supersolar  $Fe/O$  abundance, we are beginning to constrain cosmological models, favoring those which predict larger galaxy ages at a given  $z$ .

In the near future, Fe abundance measurements of larger samples of high- $z$  quasars may provide another valuable path to measure cosmological parameters (Hamann & Ferland 1993).

This work is based on observations obtained with *XMM-Newton*, an ESA science mission with instruments and contributions directly funded by ESA Member States and the USA (NASA). We thank the project scientist, Fred Jansen, for granting directors discretionary time for the long observation presented here, and the Science Operation Center in Villafranca for carrying out the observations efficiently. On the German side, the *XMM-Newton* project is supported by the Bundesministerium für Bildung und Forschung/Deutsches Zentrum für Luft- und Raumfahrt (BMBF/DLR), the Max-Planck Society and the Heidenhain-Stiftung. We thank Sarah Gallagher for making available to us the *Chandra* spectrum of APM 08279+5255, and Gary Ferland for providing *Cloudy*. We acknowledge helpful discussions with H. Böhringer, C. Done, P. Petitjean, Th. Boller, W. Brinkmann, D. Porquet and Weimin Yuan. We thank the referee, Martin Elvis, for very helpful comments.

## REFERENCES

- Done, C., Mulchaey, J. S., Mushotzky, R. F., Arnaud, K. A., 1992, *ApJ*, 395, 275
- Egami, E., Neugebauer, G., Soifer, B. T., Matthews, K., Ressler, M., Becklin, E. E., Murphy, T. W., Jr., Dale, D. A., 2000, *ApJ*, 535, 561
- Ellison, S. L., Lewis, G. F., Pettini, M., 1999, *PASP*, 111, 946
- Elvis, M., 2000, *ApJ*, 545, 63
- Ferland, G. J., 1993, *Hazy*, a Brief Introduction to CLOUDY (Lexington: Univ. Kentucky Dept. Phys. Astron. Int. Rep.
- Gallagher, S. C., Brandt, W. N., Chartas, G., Garmire, G. P., 2002, *ApJ*, 567, 37
- Hamann, F., 1998, *ApJ*, 500, 798
- Hamann, F., Ferland, G.J., 1993, *ApJ*, 418, 11

- Ibata, R. A., Lewis, G. F., Irwin, M. J.; Lehar, J., Totten, E. J., 1999, ApJ, 524, L95
- Irwin, M. J., Ibata, R. A., Lewis, G. F.; Totten, E. J., 1998, ApJ, 505, 529
- Komossa, S., 1999, in ASCA/ROSAT workshop on AGN and the X-ray Background, ed. T. Takahashi & H. Inoue (ISAS Rep. 149; Tokyo: ISAS) [astro-ph/0001263]
- Ledoux, C., Theodore, B., Petitjean, P., Bremer, M. N., Lewis, G. F., Ibata, R. A., Irwin, M. J., Totten, E. J., 1998, A&A, 339, L77
- Lewis, G. F., Chapman, S. C., Ibata, R. A., Irwin, M. J., Totten, E. J., 1998, ApJ505, L1
- Mathur, S., Wilkes, B., Elvis, M., Fiore F., 1994, ApJ, 434, 493
- Murray, N., Chiang, J., 1995, ApJ, 454, L105
- Schartel, N., Komossa, S., Brinkmann, W., Fink, H.H., Trümper, J., Wamsteker, W., 1997, A&A, 320, 421
- Srianand, R., Petitjean, P., 2000, A&A, 357, 414
- Verner, D. A., Yakovlev D. G., 1995, A&ASupplement Series, 109, 125

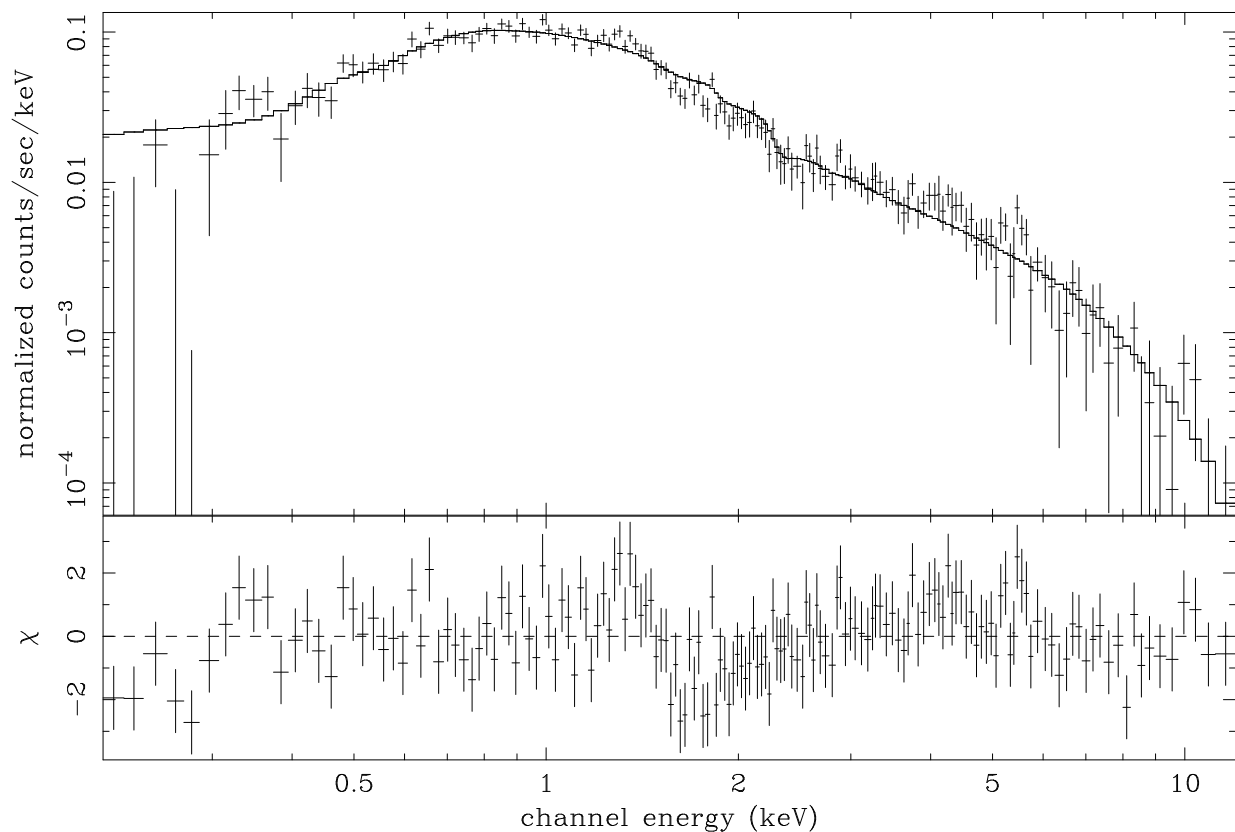


Fig. 1.— X-ray spectrum of APM 08279+5255 taken with the *XMM-Newton* pn-CCD camera, fit with a simple power law model absorbed by neutral gas in our own Galaxy as well as associated with the source. This fit is statistically not acceptable; residuals are shown below the curve.

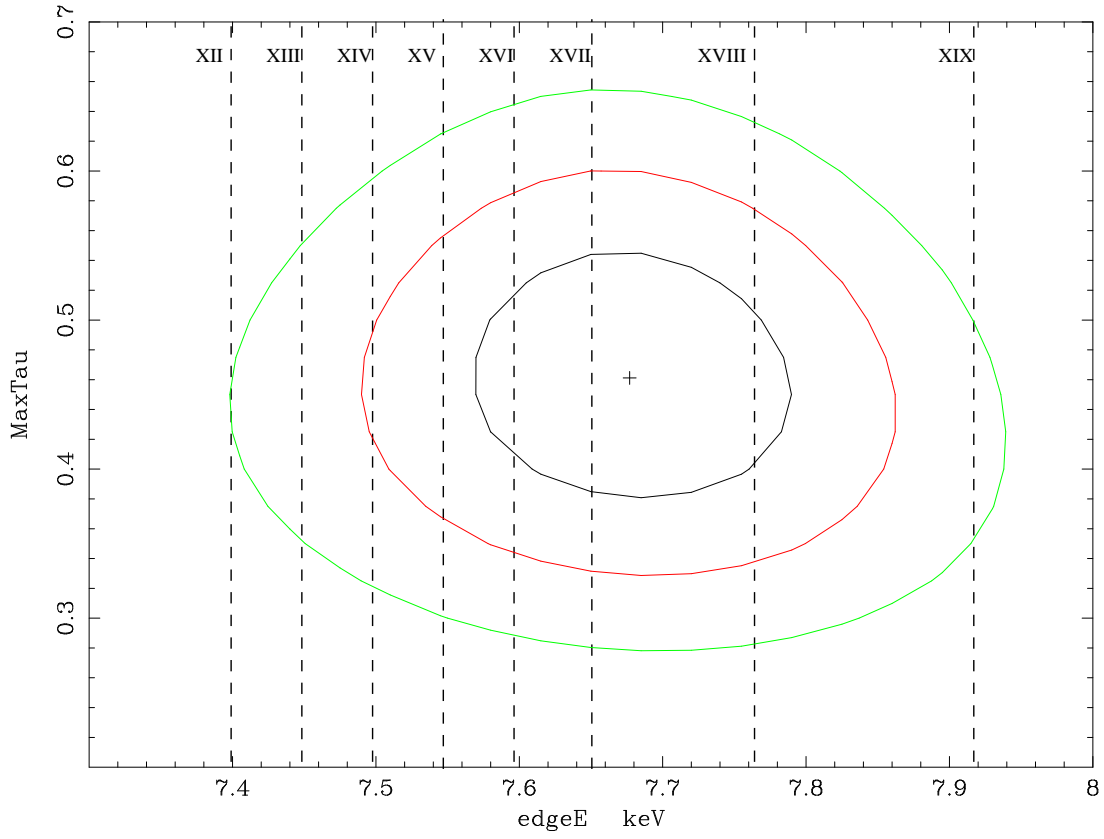


Fig. 2.— Confidence contours of the edge energy versus the optical depth of the edge. Contours are given for 1, 2 and  $3\sigma$  deviations from the best fit. The dashed vertical lines refer to the Fe-K edges for the specified ionic species.

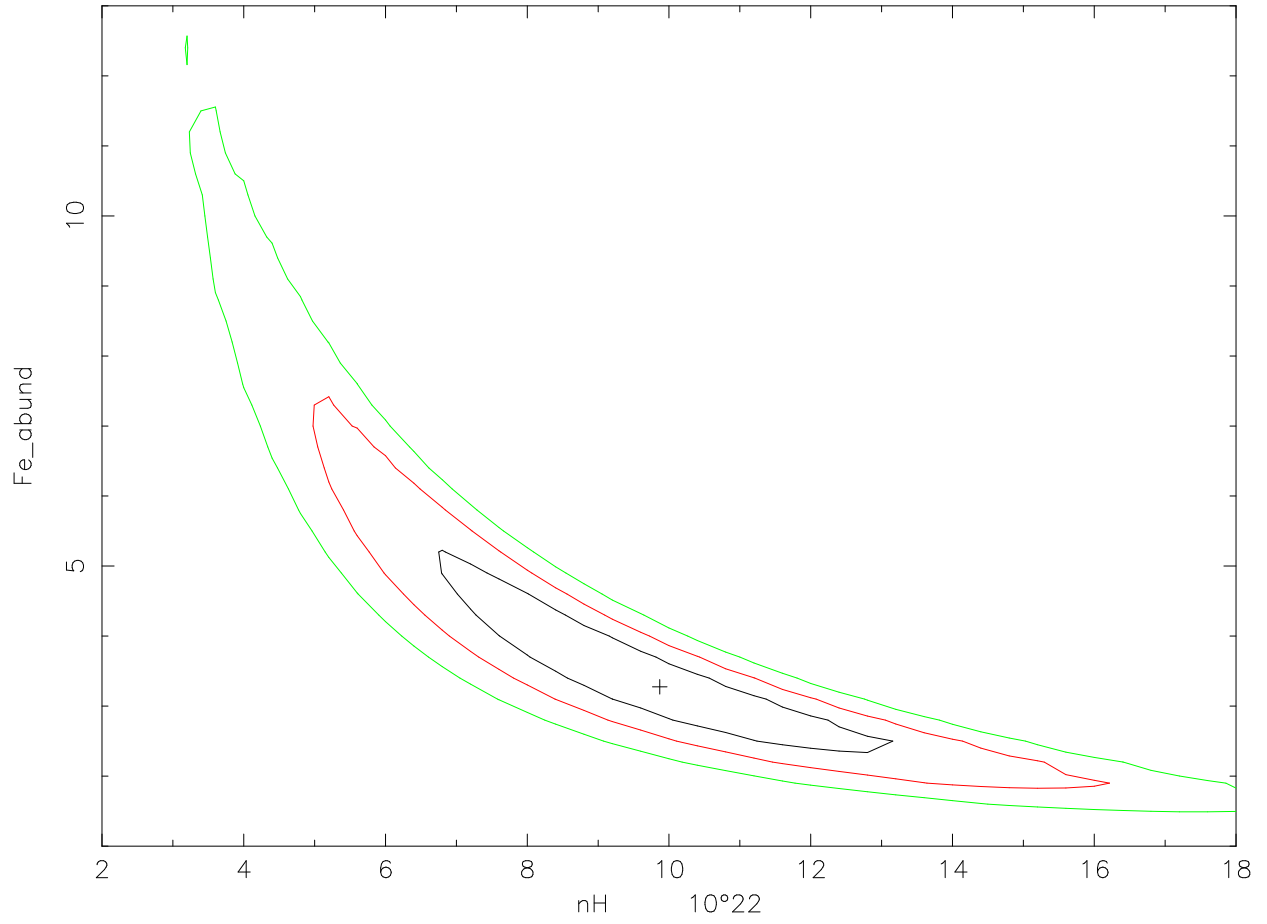


Fig. 3.— Confidence contours of the hydrogen column density  $N_H$  versus the iron abundance  $Fe/O$  in an ionized absorber (*absori*) fit.

Table 1: Observing log for APM 08279+5255.

ID	Start Date [UT]	End Date [UT]	Filter	Exposure [s]	Instrument
CXO1	11.10.2000 16:13	11.10.2000 19:24		9137	ACIS-I
XMM1	30.10.2001 02:50	30.10.2001 07:35	medium	16523	EPIC
XMM2	28.04.2002 17:07	29.04.2002 21:36	medium	102274	EPIC

Table 2. Spectral fit results.

ID	$N_H^a$	$\Gamma$	Norm <sup>b</sup>	$E_{edge}$	$\tau$	$\xi^c$	$Fe/H$	$\chi^2_{red}$	d.o.f.
CXO1	5.26±0.77	1.78±0.08	1.48±0.19	...	...	...	...	1.05	51
XMM1	6.18±0.46	1.98±0.04	1.30±0.09	...	...	...	...	1.32	168
XMM2	6.92±0.32	2.04±0.03	1.30±0.05	...	...	...	...	1.32	365
CXO1	5.44±0.77	1.76±0.08	1.55±0.21	7.67±0.39	0.30±0.16	...	...	1.00	49
XMM1	6.67±0.47	1.96±0.04	1.41±0.10	7.62±0.13	0.47±0.08	...	...	1.10	165
XMM2	7.34±0.34	2.01±0.03	1.37±0.06	7.68±0.10	0.46±0.05	...	...	1.09	362
XMM1	9.1±1.4	2.00±0.04	1.44±0.11	...	...	29±23	3 <sup>d</sup>	1.14	166
XMM2	9.8±2.3	2.03±0.03	1.42±0.07	...	...	47±12	3.3±0.9	1.09	362

<sup>a</sup>absorber at  $z=3.91$  in units of  $10^{22} \text{ cm}^{-2}$  (for “*absori*”: ionized); all models include Galactic absorption.

<sup>b</sup> in  $10^{-4} \text{ ph cm}^{-2} \text{ s}^{-1} \text{ keV}^{-1}$ .

<sup>c</sup>Ionization parameter  $\xi$  from ionized absorber fit.

<sup>d</sup>fixed in fit.